PHASE COMPOSITION OF CHOSEN Mg-BASED MATERIALS DURING HYDROGEN SORPTION

Jiří ČERMÁK[1, 2], Lubomír KRÁL[1], Pavla ROUPCOVÁ[1, 3]

[1]*Institute of Physics of Materials of the CAS, Brno, Czech Republic, EU*
[2]*CEITEC-Institute of Physics of Materials of the CAS, Brno, Czech Republic, EU*
[3]*CEITEC-Brno University of Technology, FME, IMSE, Brno, Czech Republic, EU*

Abstract

Phase transformation during hydrogen sorption was investigated in ten chosen magnesium-based hydrogen storage (HS) materials. Chemical composition of the materials consisted of Mg, as a principal hydrogen-binding element, additive X and amorphous carbon (CB), as an anti-sticking component. In order to assess the effect of X itself upon the structure, values of concentration of both X and CB were fixed to about 12 wt. %. The influence of X = Mg_2Si, Mg_2Ge, $Mg_{17}Al_{12}$, Mg_5Ga_2, NaCl, LiCl, NaF, LiF and two combinations Ni+$Mg_{17}Al_{12}$ and Ni+Mg_2Si upon the changes in phase composition was tested. Phase content in HS materials was observed (i) after the intensive ball milling (BM), (ii) after the BM followed by hydrogen charging at 623 K and (iii) after the BM and one hydrogen charging/discharging cycle (C/D) at temperature 623 K. The study was carried out by SEM and XRD. It was found that, the C/D is approximately structurally reversible for X = Mg_2Ge, $Mg_{17}Al_{12}$, NaF and LiF. However, additives X = $Mg_{17}Al_{12}$ and NaF decompose already during the BM. In alloys with combination of Ni with $Mg_{17}Al_{12}$, new phases Ni_mAl_n are formed. Phase composition changed during C/D for X = Mg_2Si Mg_5Ga_2 and Ni+Mg_2Si due to equilibration of phases composition. Observed structure changes of HS materials with chloride ionic additives NaCl and LiCl are, most likely caused by the relatively strong affinity between Mg and Cl. Hydrogen storage capacity of all studied alloys was 6.0 ± 0.3 wt. % H_2.

Keywords: Hydrogen storage, Mg alloys, carbon black

1. INTRODUCTION

Mg-based alloys are promising materials for HS applications [1,2]. The principal HS phase in alloys of this type is MgH_2 hydride. This phase shows high HS capacity (7.7 wt. % H_2) and excellent cycling behavior. The substantial drawback is its high thermodynamic stability, which implies high operation temperatures (starting from approximately 573 K). Much research work was devoted to decrease the high stability of MgH_2 [see, e.g., in 3], i.e. to increase hydrogen pressure in equilibrium, p_{eq}, above the Mg hydride. This would shift working temperatures of HS reservoirs down to desired values (to some 400 K). However, this proved to be an extraordinary difficult task. After a considerable research effort, only moderate success was reached in this respect. Instead of improvement of the hydrogen sorption dynamics, rather an acceleration of sorption process stands in the focus of research groups in the last years. of course, the two aspects are closely interconnected, but the smoothing the kinetic paths of the process seem to be easier task then to affect effectively the driving forces. The main ways how to achieve the target seem to be the catalysis of partial sorption steps [4] and nanosizing [5].

In the present work, structure of ball-milled (BM) HS blend of Mg with chosen additives during the C/D cycle was investigated. Five types of additives were tested: (i) Mg intermetallics formed by two elements from 13th group (Mg_2Ge, Mg_2Si), (ii) by two elements of 14th group (Mg_5Ga_2, $Mg_{17}Al_{12}$), (iii) additives formed by two combination Ni+$Mg_{17}Al_{12}$ and Ni+Mg_2Si (iv) two simple fluorides with Na^+ and Li^+ (NaF, LiF), and (v) two chlorides with the same kations (NaCl, LiCl). Expectation of beneficial effect of the intermetallics with elements from 13th and 14th group upon the C/D kinetics was based on results published in [6], synergy of those elements

and Ni can be expected with regard to results from [7] and improvement of C/D kinetic by anions F^-, Cl^- and/or cations Na^+, Li^+ may be expected from results published in [8-10]. Sufficient nanosizing of the BM blend was assured by introduction of carbon black (CB) [11].

2. EXPERIMENTAL

Samples were made from pure components Mg(purity: 3N8), Ge(5N), Si(6N), Ga(4N), Al(5N), Ni(3N), LiF, LiCl, NaF, NaCl (all halides >2N) and CB (2N). Intermetallics Mg_2Si and Mg_2Ge were prepared by mechanical alloying in form of powders. Compounds $Mg_{17}Al_{12}$ and Mg_5Ga_2 were induction melted in pure Ar(4N) and grinded into form of splinters and halides and CB were purchased as fine powders. All the additives were mixed with splinters of Mg and ball milled (BM) in hydrogen atmosphere (6N) using Fritsch Pulverisette6 ball-mill. Two HS samples were prepared with admixture of fine powder of Ni. The mass ratio of the milling balls to the milled blend was about 60 and the milling cycle - 10 min milling/50 min cooling - was repeated 90 times. Hydrogen charging under pressure p = 2.5 MPa and discharging was carried out using Sieverts-type gas sorption analyzer PCT-Pro Setaram Instrumentation at constant temperature 623 K. All manipulations of the milled blend were done in the glove box in protective Ar atmosphere. Nominal chemical composition of ball milled batches is listed in **Table1**.

Table 1 Experimental samples

Sample label	Nominal composition of batch (wt. %)	Chemical composition (wt. %)
Si	76.36 Mg - 10.25 Mg_2Si - 13.39 CB	81.79 Mg - 4.82 Si - 13.39 C
Ge	75.28 Mg - 12.61 Mg_2Ge - 12.11 CB	80.32 Mg - 7.57 Ge 12.11 C
Al	76.58 Mg - 10.40 $Mg_{17}Al_{12}$ - 13.02 CB	82.48 Mg - 4.5 Al - 13.02 C
Ga	81.61 Mg - 10.91 Mg_5Ga_2 - 7.48 CB	86.72 Mg - 5.80 Ga -7.48 C
NiSi	71.87 Mg - 3.26 Ni - 12.47 Mg_2Si - 12.40 CB	79.76 Mg - 3.26 Ni - 4.58 Si - 12.40 C
NiAl	72.37 Mg - 2.53 Ni - 12.84 $Mg_{17}Al_{12}$ - 12.31 CB	79.82 Mg - 2.53 Ni - 5.39 Al - 12.31 C
LiF	74.04 Mg - 13.18 LiF - 12.78 CB	74.04 Mg - 3.35 Li - 9.65 F 12.78 C
NaF	74.81 Mg - 12.41 NaF - 12.78 CB	74.81 Mg - 6.81 Na - 5.60 F - 12.78 C
LiCl	75.94 Mg - 11.57 LiCl - 12.49 CB	75,94 Mg - 1.89 Li - 9.68 Cl - 12.49 C
NaCl	74.61 Mg - 12.99 NaCl -12.40 CB	74.60 Mg - 5.20 Na -7.80 CL - 12.40 C

Phase composition of samples was obtained by XRD with the help of the X'Pert Pro MPD device using CoKa radiation and the results were interpreted (Rietveld analysis) with the HighScore Plus SW and ICSD databases. Accuracy of phase composition was about 1.5 wt. %. Morphology of milled samples, average chemical composition and chemical maps were observed by SEM TESCAN LYRA3 equipped with X-max80 EDS in the area approximately 300 × 500 μm containing about 10^2 grains. Accuracy of average concentration of substitution elements (except for Li) was within 1.5 wt%.

Due to considerable uncertainty in estimation of content of amorphous phase (AM) by XRD, c_{AM}, the value of c_{AM} was fixed to known concentration of CB, c_{CB}, and, due to similar reasons, for the carbon concentration, c_C, in SEM analyses, the known value $c_{AM} = c_C$ was taken (see **Table 1**). Concentration of hydrogen was measured by sorption experiment (c_H = 6.0 ± 0.3 wt. % H_2 in all cases). For Li concentration, c_{Li}, in LiF-containing samples the value $c_{Li} = 0.36537 \times c_F$ and for, c_{Li}, in LiCl-containing samples the value $c_{Li} = 0.1957 \times c_{Cl}$ was taken, where concentrations c_F and c_{Cl} were obtained by SEM.

3. RESULTS AND DISCUSSION

3.1. Morphology

Morphology of all samples after the BM, its change after C and after the D steps follows very similar evolution scheme. It can be illustrated by the sample Ge. The structure of Ge after BM is shown in **Figure 1a**, where relatively smooth grains of size typically between 5 and 50 μm can be seen. These grains composed principally of solid solution (Mg) transform during C to hydride phase and their appearance becomes fragmented - **Figure 1b**. After D, when the hydrided phase(s) transformed back to hydride-free components, the fragmented structure persists and, moreover, additional transversal cracks of great grains appear - **Figure 1c**.

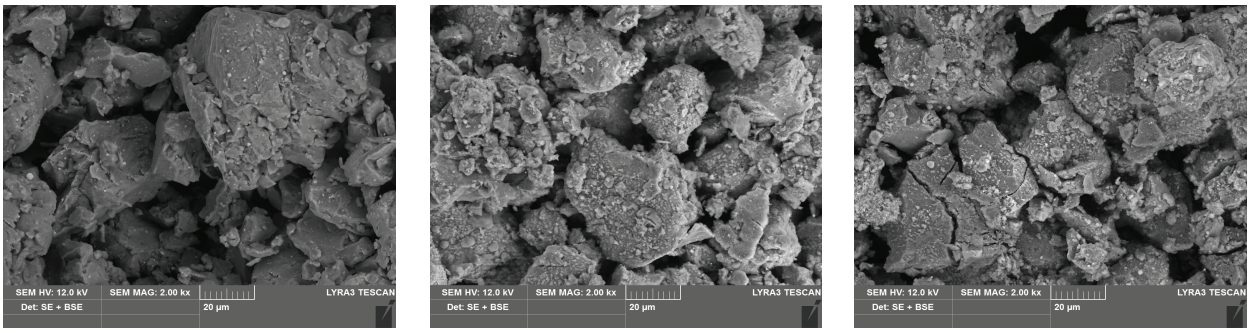

a **b** **c**

Figure 1 Typical morphology of samples after BM (a), C (b) and D (c). Sample Ge.

Fine bright particles of size about 1 μm (for Ge, see in **Figure 1a**) were identified as impurities with traces of Ti, Al, W and Fe. Concentration of these elements, was lower than 1 wt. %, and therefore it was neglected in SEM analyses.

3.2. XRD measurements

XRD patterns were measured for each sample in BM, C and D states. The obtained data could be classified qualitatively into two considerably different groups. The first typical behavior can be described by the scheme: c_{AM} in BM ≅ c_{AM} in C ≅ c_{AM} in D with c_{AM} ≅ c_{CB} (c_{AM} stands for concentration of amorphous phase from SEM analysis, c_{CB} is known concentration of carbon black). This type of behavior was observed in all alloys except for chloride-containing samples. The samples modified by chlorides (LiCl and NaCl) on the other hand, formed the other group where the measured content of AM was very high, especially in BM and D. The typical XRD patterns are exemplified in **Figure 2** for Mg_2Ge and NaCl. No carbides were detected in any sample; the components, which content was below 1 % were neglected.

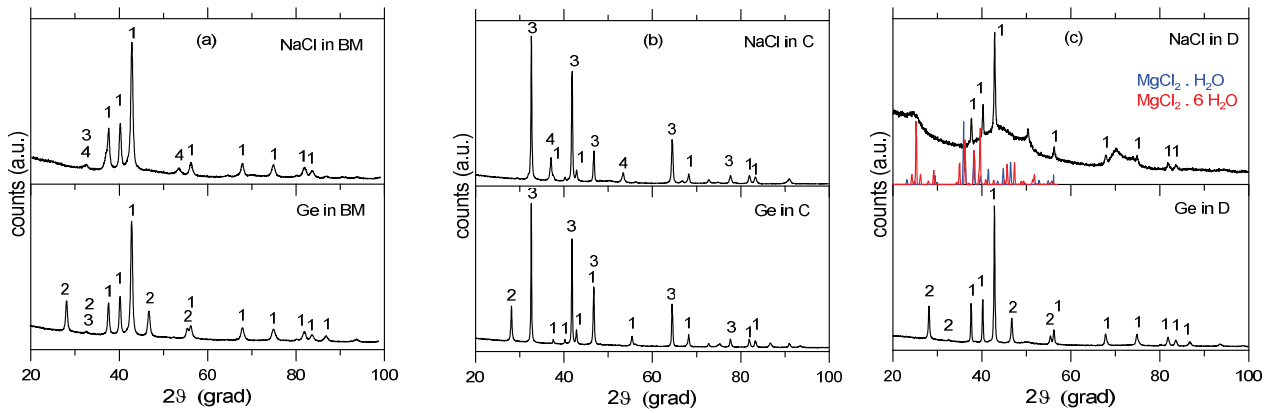

Figure 2 Two types of XRD patterns (exemplified by Ge and NaCl) in states BM (a), C (b) and D (c). 1-(Mg), 2-Mg_2Ge, 3-MgH_2, 4-NaCl. Patterns in color in (c) - magnesium chlorides [13].

3.3. Observed structure transformations - survey of results and discussion

Sample Si. After BM (phases: 79(Mg)-4Mg_2Si-2Si-2αMgH_2-13AM; elements: 84Mg-3Si-13C), Si was present both as regularly dispersed fine particles of Mg_2Si and as scattered elemental Si in the form of particles of size up to 1 μm. Separate XRD analysis of ball milled blend Mg+Si showed that the BM produced Mg_2Si compound only up to about 21 %. This explained observed differences between nominal and measured phase composition in Si sample. Presence of αMgH_2 is a consequence of BM in H_2. Chemical analysis agreed well with the nominal values (**Table** 1) within 3 wt.% (2×1.5 %). Carbon was distributed regularly. After C (78αMgH_2-9 Mg_2Si-13AM; 78Mg-3Si-13C-6H), low-pressure alpha hydride phase appeared, all elemental Si reacted with Mg and formed particles Mg_2Si (size up to 2 μm). In D state (76(Mg)-11 Mg_2Si-13AM; 84Mg-3Si-13C), particles Mg_2Si (size up to 2 μm) persisted.

Sample Ge. After BM (75(Mg)-12Mg_2Ge-13CB; 81Mg-7Ge-12AM), Mg_2Ge particles (~5 μm) were observed, C was uniformly distributed, chemical concentration agreed with nominal composition. After C (70αMgH_2-11Mg_2Ge-7(Mg)-12AM; 78Mg-5Ge-11C-6H), Mg_2Ge particles become less distinctly confined. After D (75(Mg)-13Mg_2Ge-12AMB; 83Mg-5Ge-12C), the original state was restored.

Sample Al. After BM (83(Mg)-3$Mg_{1.95}Al_{0.05}$-1MgH_2-13AM; 82Mg-5Al-13C), no $Mg_{17}Al_{12}$ phase was detected. It seems that it was decayed during BM and the products entered (Mg) phase. Al is distributed approximately uniformly; slightly higher Al concentration can be detected in $Mg_{1.95}Al_{0.05}$ particles (size between 1 and 10 μm). After C (74αMgH_2-13(Mg)-13AM; 79Mg-3Al-12C-6H), low-pressure hydride αMgH_2 appeared, presence of (Mg) solid solution is a consequence of incomplete charging. After D (86(Mg)-1MgH_2-13AM; 82Mg-5Al-13C), the state observed before after BM was restored.

Sample Ga. After BM (86(Mg-14AM; 86Mg-7Ga-7C), all components were uniformly scattered. Mg_5Ga_2 phase decomposed during BM and the decay products entered the AM and partly also the (Mg). After C (86βMgH_2-4Mg_5Ga_2-3Mg_2Ga-7AM; 85Mg-2Ga-7C-6H), one of high pressure phases [12] was formed (β). Loci (~1μ) with significantly higher concentration of Ga were observed, which were identified as two Mg_mGa_n phases. They precipitated from AM. After D (85((Mg)-8Mg_5Ga_2-7AM; 88Mg-5Ga-7C), Mg_5Ga_2 particles persisted.

Sample NiSi. After BM (77(Mg)-4Mg_2Si-1Ni-2Si-5αMgH_2-12AM; 80Mg-4Ni-4Si-12C), Si particles (~2 μm) that anti-coincided with Mg were observed. Mg_2Si not completely formed (similarly as in sample Si above). After C (76αMgH_2-1(Mg)-10Mg_2Si-1Ni-12AM, 77Mg-2Ni-3Si-12C-6H), Formation of Mg_2Si phase completed (particles ~2-3 μm). After D (74(Mg)-13Mg_2Si-1$Mg_2NiH_{3.8}$-12AM; 81Mg-3Ni-4Si-12C), particles of Mg_2Si were restored, trace amount of ternary Mg-Ni hydride (particles ~3 μm) was a residuum after the C.

Sample NiAl. After BM (85(Mg)-1$Ni_{0.89}Al_1$-1Ni-1αMgH_2-12AM; 80Mg-3Ni-5Al-12C), the $Mg_{17}Al_{12}$ decayed and the residuals entered (Mg). After C (82αMgH_2-1(Mg)-5N_2Al_3-2AM; 77Mg-2Ni-3Al-12C-6H), Mg was mostly bound in MgH_2, Sporadic Mg particles were also observed. Al was scattered uniformly; no localized phase particles composed of Ni, Al and Mg were observed. Diffuse coincidence between Al and Ni seems to be more pronounced than that between Al and Mg. After D (83(Mg)-4Ni_2Al_3-1NiAl-12AM; 80Mg-3Ni-5Al-12C), new-formed phases Ni_mAl_n replaced completely originally introduced phase $Mg_{17}Al_{12}$ in hydrogen-free sample.

Sample LiF. After BM (75(Mg)-12LiF-13AM; 75Mg-3Li-9F-13C), Small particles LiF (~3 μm) were observed on the surface of great Mg grains. C was scattered uniformly. After C (83βMgH_2-2LiF-2(Mg)-13AM; 68Mg-4Li-10F-12C-6H), the identity of LiF phase remained even after the hydrogen charging. One of high pressure phases of MgH_2 (β phase) was formed by BM. (Mg) phase was a consequence of incomplete charging. After D (75(Mg)-11LiF-1MgH_2-13AM; 73Mg-4Li-10F-13C), the original state observed after BM was almost exactly restored.

Sample NaF. After BM (80(Mg)-7NaM$gF_{1.17}H_{1.83}$-13AM; 75Mg-6Na-6F-13C), NaF decomposed during BM and the decay products entered the (Mg) phase. A small fraction of ternary hydride was formed. All chemical components are scattered uniformly. After C (84βMgH_2-1$NaMgH_3$-2(Mg)-13AM; 74Mg-5Na-3F-12C-6H), high

pressure hydride βMgH$_2$ was formed, ternary hydride changed its composition and F remained solved in major phases. After D (80(Mg)-7NaMgF$_{1.17}$H$_{1.83}$-13AM; 79Mg-4Na-4F-13C), the original state was approached, observed after BM.

Sample LiCl. After BM (73(Mg)-11LiCl-4βMgH$_2$-12AM; 76Mg-2Li-10Cl-12C), both phase and chemical composition agree approximatelly with nominal values; high pressure βMgH$_2$ was formed. After C (72αMgH$_2$-15Li-1(Mg)-12AM; 67Mg-2Li-12Cl-12C-6H), LiCl was found completely decayed. Cl entered hydride phase and Li precipitated in elemental form. After D (2(Mg)-98AM; 73Mg-2Li-12Cl-12C), AM phase grew significantly. It was most likely due to interaction of Cl with Mg [13] that produced finally extremely fine (almost amorphous) phase. Positions of chlorides lines are plotted in **Figure 2c.** In case of fine structure they may broaden and superimpose over LiCl pattern. In results, they may be involved in overall AM phase.

Sample NaCl. After BM (77(Mg)-8NaCl-3αMgH$_2$-12AM; 75Mg-5Na-8Cl-12C), NaCl phase was found partly decomposed; the decay products entered (Mg) phase. After C (74αMgH$_2$-9NaCl-5Mg-12AM; 70Mg-5Na-7Cl-12C-6H), NaCl phase remained also after hydrogen charging. After D (10(Mg)-90AM; 74Mg-5Na-9Cl-12C), NaCl phase decayed and the transformation products entered the phase that behaves as AM. AM contains also prevailing fraction of Mg. Most likely, this is a result of fragmentation of MgH$_2$ into very fine particles during interaction of Mg with Cl - reasoning is similar as in the case of sample LiCl.

3.4. Observed structure transformations - summary

Chemical composition of all samples in states BM and D are reasonably equal to elements nominal concentrations in milling batches. In sample Ge, the added phase Mg$_2$Ge is unaffected by C/D cycle. In samples Si and NiSi the phase Mg$_2$Si behaves similarly to Mg$_2$Ge - its lower content in the BM state is caused by its incomplete formation in the beginning of the C/D cycle. Phase Mg$_{17}$Al$_{12}$ in samples Al and NiAl decayed already during BM and does not reform during D. Moreover, Al from decayed Mg$_{17}$Al$_{12}$ forms very stable phases Ni$_m$Al$_n$ in sample NiAl. Added phases in samples Ga and LiF decay during BM, but during D, they are (partly) reformed. In samples NaF, LiCl and NaCl the added phases decay during BM, but they do not restore in D state. In samples LiCl and NaCl, significantly high fraction of AM was observed after the C/D cycle. Hydrogen charging of samples with halides and with Mg$_5$Ga$_2$ led to a formation of high pressure phase of Mg hydride (βMgH$_2$).

4. CONCLUSION

Different structure evolution schemes were observed in Mg-based HS mixtures modified by chosen admixtures that could be effective in HS behavior. It was found that composition modified by combination of Ni and Mg$_{17}$Al$_{12}$, forms Ni$_m$Al$_n$ phase(s), which decreased their beneficial catalytic effect. On the other hand, admixture of halides (NaF, NaCl, LiF and LiCl), especially chlorides that support formation of AM, may be good components of HS Mg-based alloys. Sorption experiments that may support these conclusions are running.

ACKNOWLEDGEMENTS

This work was supported by project of Czech Science Foundation No. 17-21683S.

REFERENCES

[1] HUOT, J. Metal Hydrides. In: HIRSCHER, Michael ed. *Handbook of hydrogen storage* Weinheim: WILEY-VCH Verlag GmbH &Co. KGaA, 2010, pp. 81-110.

[2] CRIVELO, J.-C., DENYS, R.V., DORNHEIM, M., FELDERHOFF, M., GRANT, D.M., HUOT, J., JENSEN, T.R., deJONGH, P., LATROCHE, M., WALKER, G.S., WEBB, C.J. and YARTYS, V.A. Mg-based compounds for hydrogen storage. *Applied Phys. A.* 2016. vol.85, pp 122-139.

[3] WANG, H., LIN, H.J., CAI, W.T., OUYANG, L.Y. and ZHU, M. Tuning kinetics and thermodynamics of hydrogen storage in light metal element based systems-A review of recent progress. *J. Alloys Compd.* 2016. vol. 658, pp.280-300.

[4] Li, Q., LIN, Q., CHOU, K-C. and JIANG, L. A study on the hydriding-dehydriding kinetics of $Mg_{1.9}Al_{0.1}Ni$. *J. Mater Sci.* 2001. vol. 39, pp.61-65.

[5] YHU, Y., LIU, Z., YANG, Y., GU, H., LI, L. and CAI, M. Hydrogen storage properties of Mg-Ni-C system hydrogen storage materials prepared by hydriding combustion synthesis and mechanical milling. *Int. J. Hydrogen energy*. 2010. vol. 35, pp.6350-6355.

[6] CERMAK, J. and KRAL, L. Alloying of Mg/Mg_2Ni eutectic by chosen non-hydride forming elements: Relation between segregation of the third element and hydride storage capacity. *J. Power Sources*. 2012. vol. 197, pp.116-120.

[7] CERMAK, J. and KRAL, L. Hydrogen diffusion in Mg-H and Mg-Ni-H alloys. *Acta Mater.* 2008. Vol. 56, pp.2677-2686.

[8] VAJO, J.,J., MERTENS, F., AHN, C.,C., BOWMAN jr., R.,C. and FULTZ, B. Altering hydrogen storage properties by hydride destabilization through alloy formation: LiH and MgH_2 destabilized with Si. *J. Phys. Chem. B*. 2004. vol. 108, pp.13977-13983.

[9] LIU, H., WU, C., ZHOU, H., CHEN, T.,LIU, Y., WANG, X., DONG, Z., GE, H., Li, S. and YAN, M. Synergistically thermodynamic and kinetic tailoring of the hydrogen desorption properties of MgH_2 by co-addition of AlH_3 and CeF_3. *RSC Advances*. 2015. vol. 5, pp.22091-22096.

[10] LYCI, G. and SURENDRA, K., S. Structural stability of metal hydrides, alanates and borohydrates of alkali and alkali- earth elements: A review. *Int. J. hydrogen energy*. 2010. vol. 35, pp.5454-5470.

[11] CERMAK, J. and KRAL, L. Hydrogen absorption in carbon allotropes and talc. *Kovove Mater.-Metallic Mater.* 2018, vol. 56, pp.75-80.

[12] VAJEESTON, P., RAVINDRAN, P., HAUBACK, B.C., FJELLVAG, H., KJEKSHUS, A., FURUSETH, S. and HANFLAND, M. *Phys. Rev.B.* 2006. vol. 73. p.224102.

[13] HUANG, Q., LU, G., WANG, J and YU, J. Thermal decomposition mechanism of $MgCl_2.6H_2O$ and $MgCl_2.H_2O$. *J. Analyt.Appl. Pyrolysis.* 2011. vol. 91, pp. 159-164.